

Measurements of the absolute branching fractions of the doubly Cabibbo-suppressed decays

$D^+ \rightarrow K^+\pi^0$, $D^+ \rightarrow K^+\eta$ and $D^+ \rightarrow K^+\eta'$

The BESIII Collaboration



M. Ablikim¹, M. N. Achasov^{4,c}, P. Adlarson⁷⁷, X. C. Ai⁸², R. Aliberti³⁶,
A. Amoroso^{76A,76C}, Q. An^{73,59,a}, Y. Bai⁵⁸, O. Bakina³⁷, Y. Ban^{47,h}, H.-R. Bao⁶⁵,
V. Batozskaya^{1,45}, K. Begzsuren³³, N. Berger³⁶, M. Berlowski⁴⁵, M. Bertani^{29A},
D. Bettoni^{30A}, F. Bianchi^{76A,76C}, E. Bianco^{76A,76C}, A. Bortone^{76A,76C}, I. Boyko³⁷,
R. A. Briere⁵, A. Brueggemann⁷⁰, H. Cai⁷⁸, M. H. Cai^{39,k,l}, X. Cai^{1,59},
A. Calcaterra^{29A}, G. F. Cao^{1,65}, N. Cao^{1,65}, S. A. Cetin^{63A}, X. Y. Chai^{47,h},
J. F. Chang^{1,59}, G. R. Che⁴⁴, Y. Z. Che^{1,59,65}, C. H. Chen⁹, Chao Chen⁵⁶, G. Chen¹,
H. S. Chen^{1,65}, H. Y. Chen²¹, M. L. Chen^{1,59,65}, S. J. Chen⁴³, S. L. Chen⁴⁶,
S. M. Chen⁶², T. Chen^{1,65}, X. R. Chen^{32,65}, X. T. Chen^{1,65}, X. Y. Chen^{12,g},
Y. B. Chen^{1,59}, Y. Q. Chen¹⁶, Y. Q. Chen³⁵, Z. Chen²⁵, Z. J. Chen^{26,i}, Z. K. Chen⁶⁰,
S. K. Choi¹⁰, X. Chu^{12,g}, G. Cibinetto^{30A}, F. Cossio^{76C}, J. Cottee-Meldrum⁶⁴,
J. J. Cui⁵¹, H. L. Dai^{1,59}, J. P. Dai⁸⁰, A. Dbeysi¹⁹, R. E. de Boer³, D. Dedovich³⁷,
C. Q. Deng⁷⁴, Z. Y. Deng¹, A. Denig³⁶, I. Denysenko³⁷, M. Destefanis^{76A,76C},
F. De Mori^{76A,76C}, B. Ding^{68,1}, X. X. Ding^{47,h}, Y. Ding⁴¹, Y. Ding³⁵, Y. X. Ding³¹,
J. Dong^{1,59}, L. Y. Dong^{1,65}, M. Y. Dong^{1,59,65}, X. Dong⁷⁸, M. C. Du¹, S. X. Du^{12,g},
S. X. Du⁸², Y. Y. Duan⁵⁶, P. Egorov^{37,b}, G. F. Fan⁴³, J. J. Fan²⁰, Y. H. Fan⁴⁶,
J. Fang⁶⁰, J. Fang^{1,59}, S. S. Fang^{1,65}, W. X. Fang¹, Y. Q. Fang^{1,59}, R. Farinelli^{30A},
L. Fava^{76B,76C}, F. Feldbauer³, G. Felici^{29A}, C. Q. Feng^{73,59}, J. H. Feng¹⁶, L. Feng^{39,k,l},
Q. X. Feng^{39,k,l}, Y. T. Feng^{73,59}, M. Fritsch³, C. D. Fu¹, J. L. Fu⁶⁵, Y. W. Fu^{1,65},
H. Gao⁶⁵, X. B. Gao⁴², Y. Gao^{73,59}, Y. N. Gao^{47,h}, Y. N. Gao²⁰, Y. Y. Gao³¹,
S. Garbolino^{76C}, I. Garzia^{30A,30B}, P. T. Ge²⁰, Z. W. Ge⁴³, C. Geng⁶⁰,
E. M. Gersabeck⁶⁹, A. Gilman⁷¹, K. Goetzen¹³, J. D. Gong³⁵, L. Gong⁴¹,
W. X. Gong^{1,59}, W. Gradi³⁶, S. Gramigna^{30A,30B}, M. Greco^{76A,76C}, M. H. Gu^{1,59},
Y. T. Gu¹⁵, C. Y. Guan^{1,65}, A. Q. Guo³², L. B. Guo⁴², M. J. Guo⁵¹, R. P. Guo⁵⁰,
Y. P. Guo^{12,g}, A. Guskov^{37,b}, J. Gutierrez²⁸, K. L. Han⁶⁵, T. T. Han¹, F. Hanisch³,
K. D. Hao^{73,59}, X. Q. Hao²⁰, F. A. Harris⁶⁷, K. K. He⁵⁶, K. L. He^{1,65}, F. H. Heinsius³,

C. H. Heinz³⁶, Y. K. Heng^{1,59,65}, C. Herold⁶¹, P. C. Hong³⁵, G. Y. Hou^{1,65},
X. T. Hou^{1,65}, Y. R. Hou⁶⁵, Z. L. Hou¹, H. M. Hu^{1,65}, J. F. Hu^{57,j}, Q. P. Hu^{73,59},
S. L. Hu^{12,g}, T. Hu^{1,59,65}, Y. Hu¹, Z. M. Hu⁶⁰, G. S. Huang^{73,59}, K. X. Huang⁶⁰,
L. Q. Huang^{32,65}, P. Huang⁴³, X. T. Huang⁵¹, Y. P. Huang¹, Y. S. Huang⁶⁰,
T. Hussain⁷⁵, N. Hüskens³⁶, N. in der Wiesche⁷⁰, J. Jackson²⁸, Q. Ji¹, Q. P. Ji²⁰,
W. Ji^{1,65}, X. B. Ji^{1,65}, X. L. Ji^{1,59}, Y. Y. Ji⁵¹, Z. K. Jia^{73,59}, D. Jiang^{1,65}, H. B. Jiang⁷⁸,
P. C. Jiang^{47,h}, S. J. Jiang⁹, T. J. Jiang¹⁷, X. S. Jiang^{1,59,65}, Y. Jiang⁶⁵, J. B. Jiao⁵¹,
J. K. Jiao³⁵, Z. Jiao²⁴, S. Jin⁴³, Y. Jin⁶⁸, M. Q. Jing^{1,65}, X. M. Jing⁶⁵, T. Johansson⁷⁷,
S. Kabana³⁴, N. Kalantar-Nayestanaki⁶⁶, X. L. Kang⁹, X. S. Kang⁴¹, M. Kavatsyuk⁶⁶,
B. C. Ke⁸², V. Khachatryan²⁸, A. Khoukaz⁷⁰, R. Kiuchi¹, O. B. Kolcu^{63A}, B. Kopf³,
M. Kuessner³, X. Kui^{1,65}, N. Kumar²⁷, A. Kupsc^{45,77}, W. Kühn³⁸, Q. Lan⁷⁴,
W. N. Lan²⁰, T. T. Lei^{73,59}, M. Lellmann³⁶, T. Lenz³⁶, C. Li^{73,59}, C. Li⁴⁴, C. Li⁴⁸,
C. H. Li⁴⁰, C. K. Li²¹, D. M. Li⁸², F. Li^{1,59}, G. Li¹, H. B. Li^{1,65}, H. J. Li²⁰, H. N. Li^{57,j},
Hui Li⁴⁴, J. R. Li⁶², J. S. Li⁶⁰, K. Li¹, K. L. Li²⁰, K. L. Li^{39,k,l}, L. J. Li^{1,65}, Lei Li⁴⁹,
M. H. Li⁴⁴, M. R. Li^{1,65}, P. L. Li⁶⁵, P. R. Li^{39,k,l}, Q. M. Li^{1,65}, Q. X. Li⁵¹, R. Li^{18,32},
S. X. Li¹², T. Li⁵¹, T. Y. Li⁴⁴, W. D. Li^{1,65}, W. G. Li^{1,a}, X. Li^{1,65}, X. H. Li^{73,59},
X. L. Li⁵¹, X. Y. Li^{1,8}, X. Z. Li⁶⁰, Y. Li²⁰, Y. G. Li^{47,h}, Y. P. Li³⁵, Z. J. Li⁶⁰, Z. Y. Li⁸⁰,
H. Liang^{73,59}, Y. F. Liang⁵⁵, Y. T. Liang^{32,65}, G. R. Liao¹⁴, L. B. Liao⁶⁰, M. H. Liao⁶⁰,
Y. P. Liao^{1,65}, J. Libby²⁷, A. Limphirat⁶¹, C. C. Lin⁵⁶, D. X. Lin^{32,65}, L. Q. Lin⁴⁰,
T. Lin¹, B. J. Liu¹, B. X. Liu⁷⁸, C. Liu³⁵, C. X. Liu¹, F. Liu¹, F. H. Liu⁵⁴, Feng Liu⁶,
G. M. Liu^{57,j}, H. Liu^{39,k,l}, H. B. Liu¹⁵, H. H. Liu¹, H. M. Liu^{1,65}, Huihui Liu²²,
J. B. Liu^{73,59}, J. J. Liu²¹, K. Liu⁷⁴, K. Liu^{39,k,l}, K. Y. Liu⁴¹, Ke Liu²³, L. C. Liu⁴⁴,
Lu Liu⁴⁴, M. H. Liu^{12,g}, P. L. Liu¹, Q. Liu⁶⁵, S. B. Liu^{73,59}, T. Liu^{12,g}, W. K. Liu⁴⁴,
W. M. Liu^{73,59}, W. T. Liu⁴⁰, X. Liu⁴⁰, X. Liu^{39,k,l}, X. K. Liu^{39,k,l}, X. Y. Liu⁷⁸, Y. Liu⁸²,
Y. Liu⁸², Y. Liu^{39,k,l}, Y. B. Liu⁴⁴, Z. A. Liu^{1,59,65}, Z. D. Liu⁹, Z. Q. Liu⁵¹,
X. C. Lou^{1,59,65}, F. X. Lu⁶⁰, H. J. Lu²⁴, J. G. Lu^{1,59}, X. L. Lu¹⁶, Y. Lu⁷, Y. H. Lu^{1,65},
Y. P. Lu^{1,59}, Z. H. Lu^{1,65}, C. L. Luo⁴², J. R. Luo⁶⁰, J. S. Luo^{1,65}, M. X. Luo⁸¹,
T. Luo^{12,g}, X. L. Luo^{1,59}, Z. Y. Lv²³, X. R. Lyu^{65,p}, Y. F. Lyu⁴⁴, Y. H. Lyu⁸²,
F. C. Ma⁴¹, H. L. Ma¹, J. L. Ma^{1,65}, L. L. Ma⁵¹, L. R. Ma⁶⁸, Q. M. Ma¹,
R. Q. Ma^{1,65}, R. Y. Ma²⁰, T. Ma^{73,59}, X. T. Ma^{1,65}, X. Y. Ma^{1,59}, Y. M. Ma³²,
F. E. Maas¹⁹, I. MacKay⁷¹, M. Maggiora^{76A,76C}, S. Malde⁷¹, Q. A. Malik⁷⁵,
H. X. Mao^{39,k,l}, Y. J. Mao^{47,h}, Z. P. Mao¹, S. Marcello^{76A,76C}, A. Marshall⁶⁴,
F. M. Melendi^{30A,30B}, Y. H. Meng⁶⁵, Z. X. Meng⁶⁸, G. Mezzadri^{30A}, H. Miao^{1,65},
T. J. Min⁴³, R. E. Mitchell²⁸, X. H. Mo^{1,59,65}, B. Moses²⁸, N. Yu. Muchnoi^{4,c},
J. Muskalla³⁶, Y. Nefedov³⁷, F. Nerling^{19,e}, L. S. Nie²¹, I. B. Nikolaev^{4,c}, Z. Ning^{1,59},
S. Nisar^{11,m}, Q. L. Niu^{39,k,l}, W. D. Niu^{12,g}, C. Normand⁶⁴, S. L. Olsen^{10,65},
Q. Ouyang^{1,59,65}, S. Pacetti^{29B,29C}, X. Pan⁵⁶, Y. Pan⁵⁸, A. Pathak¹⁰, Y. P. Pei^{73,59},
M. Pelizaeus³, H. P. Peng^{73,59}, X. J. Peng^{39,k,l}, Y. Y. Peng^{39,k,l}, K. Peters^{13,e},
K. Petridis⁶⁴, J. L. Ping⁴², R. G. Ping^{1,65}, S. Plura³⁶, V. Prasad³⁵, F. Z. Qi¹,
H. R. Qi⁶², M. Qi⁴³, S. Qian^{1,59}, W. B. Qian⁶⁵, C. F. Qiao⁶⁵, J. H. Qiao²⁰,
J. J. Qin⁷⁴, J. L. Qin⁵⁶, L. Q. Qin¹⁴, L. Y. Qin^{73,59}, P. B. Qin⁷⁴, X. P. Qin^{12,g},
X. S. Qin⁵¹, Z. H. Qin^{1,59}, J. F. Qiu¹, Z. H. Qu⁷⁴, J. Rademacker⁶⁴, C. F. Redmer³⁶,
A. Rivetti^{76C}, M. Rolo^{76C}, G. Rong^{1,65}, S. S. Rong^{1,65}, F. Rosini^{29B,29C}, Ch. Rosner¹⁹,

M. Q. Ruan^{1,59}, N. Salone⁴⁵, A. Sarantsev^{37,d}, Y. Schelhaas³⁶, K. Schoenning⁷⁷, M. Scodeggio^{30A}, K. Y. Shan^{12,g}, W. Shan²⁵, X. Y. Shan^{73,59}, Z. J. Shang^{39,k,l}, J. F. Shangguan¹⁷, L. G. Shao^{1,65}, M. Shao^{73,59}, C. P. Shen^{12,g}, H. F. Shen^{1,8}, W. H. Shen⁶⁵, X. Y. Shen^{1,65}, B. A. Shi⁶⁵, H. Shi^{73,59}, J. L. Shi^{12,g}, J. Y. Shi¹, S. Y. Shi⁷⁴, X. Shi^{1,59}, H. L. Song^{73,59}, J. J. Song²⁰, T. Z. Song⁶⁰, W. M. Song³⁵, Y. J. Song^{12,g}, Y. X. Song^{47,h,n}, S. Sosio^{76A,76C}, S. Spataro^{76A,76C}, F. Stieler³⁶, S. S Su⁴¹, Y. J. Su⁶⁵, G. B. Sun⁷⁸, G. X. Sun¹, H. Sun⁶⁵, H. K. Sun¹, J. F. Sun²⁰, K. Sun⁶², L. Sun⁷⁸, S. S. Sun^{1,65}, T. Sun^{52,f}, Y. C. Sun⁷⁸, Y. H. Sun³¹, Y. J. Sun^{73,59}, Y. Z. Sun¹, Z. Q. Sun^{1,65}, Z. T. Sun⁵¹, C. J. Tang⁵⁵, G. Y. Tang¹, J. Tang⁶⁰, J. J. Tang^{73,59}, L. F. Tang⁴⁰, Y. A. Tang⁷⁸, L. Y. Tao⁷⁴, M. Tat⁷¹, J. X. Teng^{73,59}, J. Y. Tian^{73,59}, W. H. Tian⁶⁰, Y. Tian³², Z. F. Tian⁷⁸, I. Uman^{63B}, B. Wang⁶⁰, B. Wang¹, Bo Wang^{73,59}, C. Wang^{39,k,l}, C. Wang²⁰, Cong Wang²³, D. Y. Wang^{47,h}, H. J. Wang^{39,k,l}, J. J. Wang⁷⁸, K. Wang^{1,59}, L. L. Wang¹, L. W. Wang³⁵, M. Wang⁵¹, M. Wang^{73,59}, N. Y. Wang⁶⁵, S. Wang^{12,g}, T. Wang^{12,g}, T. J. Wang⁴⁴, W. Wang⁶⁰, W. Wang⁷⁴, W. P. Wang^{36,59,73,o}, X. Wang^{47,h}, X. F. Wang^{39,k,l}, X. J. Wang⁴⁰, X. L. Wang^{12,g}, X. N. Wang¹, Y. Wang⁶², Y. D. Wang⁴⁶, Y. F. Wang^{1,8,65}, Y. H. Wang^{39,k,l}, Y. J. Wang^{73,59}, Y. L. Wang²⁰, Y. N. Wang⁷⁸, Y. Q. Wang¹, Yaqian Wang¹⁸, Yi Wang⁶², Yuan Wang^{18,32}, Z. Wang^{1,59}, Z. L. Wang², Z. L. Wang⁷⁴, Z. Q. Wang^{12,g}, Z. Y. Wang^{1,65}, D. H. Wei¹⁴, H. R. Wei⁴⁴, F. Weidner⁷⁰, S. P. Wen¹, Y. R. Wen⁴⁰, U. Wiedner³, G. Wilkinson⁷¹, M. Wolke⁷⁷, C. Wu⁴⁰, J. F. Wu^{1,8}, L. H. Wu¹, L. J. Wu²⁰, L. J. Wu^{1,65}, Lianjie Wu²⁰, S. G. Wu^{1,65}, S. M. Wu⁶⁵, X. Wu^{12,g}, X. H. Wu³⁵, Y. J. Wu³², Z. Wu^{1,59}, L. Xia^{73,59}, X. M. Xian⁴⁰, B. H. Xiang^{1,65}, D. Xiao^{39,k,l}, G. Y. Xiao⁴³, H. Xiao⁷⁴, Y. L. Xiao^{12,g}, Z. J. Xiao⁴², C. Xie⁴³, K. J. Xie^{1,65}, X. H. Xie^{47,h}, Y. Xie⁵¹, Y. G. Xie^{1,59}, Y. H. Xie⁶, Z. P. Xie^{73,59}, T. Y. Xing^{1,65}, C. F. Xu^{1,65}, C. J. Xu⁶⁰, G. F. Xu¹, H. Y. Xu^{68,2}, H. Y. Xu², M. Xu^{73,59}, Q. J. Xu¹⁷, Q. N. Xu³¹, T. D. Xu⁷⁴, W. Xu¹, W. L. Xu⁶⁸, X. P. Xu⁵⁶, Y. Xu⁴¹, Y. Xu^{12,g}, Y. C. Xu⁷⁹, Z. S. Xu⁶⁵, F. Yan^{12,g}, H. Y. Yan⁴⁰, L. Yan^{12,g}, W. B. Yan^{73,59}, W. C. Yan⁸², W. H. Yan⁶, W. P. Yan²⁰, X. Q. Yan^{1,65}, H. J. Yang^{52,f}, H. L. Yang³⁵, H. X. Yang¹, J. H. Yang⁴³, R. J. Yang²⁰, T. Yang¹, Y. Yang^{12,g}, Y. F. Yang⁴⁴, Y. H. Yang⁴³, Y. Q. Yang⁹, Y. X. Yang^{1,65}, Y. Z. Yang²⁰, M. Ye^{1,59}, M. H. Ye^{8,a}, Z. J. Ye^{57,j}, Junhao Yin⁴⁴, Z. Y. You⁶⁰, B. X. Yu^{1,59,65}, C. X. Yu⁴⁴, G. Yu¹³, J. S. Yu^{26,i}, L. Q. Yu^{12,g}, M. C. Yu⁴¹, T. Yu⁷⁴, X. D. Yu^{47,h}, Y. C. Yu⁸², C. Z. Yuan^{1,65}, H. Yuan^{1,65}, J. Yuan³⁵, J. Yuan⁴⁶, L. Yuan², S. C. Yuan^{1,65}, X. Q. Yuan¹, Y. Yuan^{1,65}, Z. Y. Yuan⁶⁰, C. X. Yue⁴⁰, Ying Yue²⁰, A. A. Zafar⁷⁵, S. H. Zeng^{64A,64B,64C,64D}, X. Zeng^{12,g}, Y. Zeng^{26,i}, Y. J. Zeng^{1,65}, Y. J. Zeng⁶⁰, X. Y. Zhai³⁵, Y. H. Zhan⁶⁰, A. Q. Zhang^{1,65}, B. L. Zhang^{1,65}, B. X. Zhang¹, D. H. Zhang⁴⁴, G. Y. Zhang²⁰, G. Y. Zhang^{1,65}, H. Zhang^{73,59}, H. Zhang⁸², H. C. Zhang^{1,59,65}, H. H. Zhang⁶⁰, H. Q. Zhang^{1,59,65}, H. R. Zhang^{73,59}, H. Y. Zhang^{1,59}, J. Zhang⁶⁰, J. Zhang⁸², J. J. Zhang⁵³, J. L. Zhang²¹, J. Q. Zhang⁴², J. S. Zhang^{12,g}, J. W. Zhang^{1,59,65}, J. X. Zhang^{39,k,l}, J. Y. Zhang¹, J. Z. Zhang^{1,65}, Jianyu Zhang⁶⁵, L. M. Zhang⁶², Lei Zhang⁴³, N. Zhang⁸², P. Zhang^{1,8}, Q. Zhang²⁰, Q. Y. Zhang³⁵, R. Y. Zhang^{39,k,l}, S. H. Zhang^{1,65}, Shulei Zhang^{26,i}, X. M. Zhang¹, X. Y. Zhang⁴¹, X. Y. Zhang⁵¹, Y. Zhang⁷⁴, Y. Zhang¹, Y. T. Zhang⁸²,

Y. H. Zhang^{1,59}, Y. M. Zhang⁴⁰, Y. P. Zhang^{73,59}, Z. D. Zhang¹, Z. H. Zhang¹,
Z. L. Zhang⁵⁶, Z. L. Zhang³⁵, Z. X. Zhang²⁰, Z. Y. Zhang⁴⁴, Z. Y. Zhang⁷⁸, Z. Z.
Zhang⁴⁶, Zh. Zh. Zhang²⁰, G. Zhao¹, J. Y. Zhao^{1,65}, J. Z. Zhao^{1,59}, L. Zhao^{73,59},
L. Zhao¹, M. G. Zhao⁴⁴, N. Zhao⁸⁰, R. P. Zhao⁶⁵, S. J. Zhao⁸², Y. B. Zhao^{1,59},
Y. L. Zhao⁵⁶, Y. X. Zhao^{32,65}, Z. G. Zhao^{73,59}, A. Zhemchugov^{37,b}, B. Zheng⁷⁴,
B. M. Zheng³⁵, J. P. Zheng^{1,59}, W. J. Zheng^{1,65}, X. R. Zheng²⁰, Y. H. Zheng^{65,p},
B. Zhong⁴², C. Zhong²⁰, H. Zhou^{36,51,o}, J. Q. Zhou³⁵, J. Y. Zhou³⁵, S. Zhou⁶,
X. Zhou⁷⁸, X. K. Zhou⁶, X. R. Zhou^{73,59}, X. Y. Zhou⁴⁰, Y. X. Zhou⁷⁹, Y. Z. Zhou^{12,g},
A. N. Zhu⁶⁵, J. Zhu⁴⁴, K. Zhu¹, K. J. Zhu^{1,59,65}, K. S. Zhu^{12,g}, L. Zhu³⁵, L. X. Zhu⁶⁵,
S. H. Zhu⁷², T. J. Zhu^{12,g}, W. D. Zhu^{12,g}, W. D. Zhu⁴², W. J. Zhu¹, W. Z. Zhu²⁰,
Y. C. Zhu^{73,59}, Z. A. Zhu^{1,65}, X. Y. Zhuang⁴⁴, J. H. Zou¹, J. Zu^{73,59}

(BESIII Collaboration)

¹ Institute of High Energy Physics, Beijing 100049, People's Republic of China

² Beihang University, Beijing 100191, People's Republic of China

³ Bochum Ruhr-University, D-44780 Bochum, Germany

⁴ Budker Institute of Nuclear Physics SB RAS (BINP), Novosibirsk 630090, Russia

⁵ Carnegie Mellon University, Pittsburgh, Pennsylvania 15213, USA

⁶ Central China Normal University, Wuhan 430079, People's Republic of China

⁷ Central South University, Changsha 410083, People's Republic of China

⁸ China Center of Advanced Science and Technology, Beijing 100190, People's Republic of China

⁹ China University of Geosciences, Wuhan 430074, People's Republic of China

¹⁰ Chung-Ang University, Seoul, 06974, Republic of Korea

¹¹ COMSATS University Islamabad, Lahore Campus, Defence Road, Off Raiwind Road, 54000 Lahore, Pakistan

¹² Fudan University, Shanghai 200433, People's Republic of China

¹³ GSI Helmholtzcentre for Heavy Ion Research GmbH, D-64291 Darmstadt, Germany

¹⁴ Guangxi Normal University, Guilin 541004, People's Republic of China

¹⁵ Guangxi University, Nanning 530004, People's Republic of China

¹⁶ Guangxi University of Science and Technology, Liuzhou 545006, People's Republic of China

¹⁷ Hangzhou Normal University, Hangzhou 310036, People's Republic of China

¹⁸ Hebei University, Baoding 071002, People's Republic of China

¹⁹ Helmholtz Institute Mainz, Staudinger Weg 18, D-55099 Mainz, Germany

²⁰ Henan Normal University, Xinxiang 453007, People's Republic of China

²¹ Henan University, Kaifeng 475004, People's Republic of China

²² Henan University of Science and Technology, Luoyang 471003, People's Republic of China

²³ Henan University of Technology, Zhengzhou 450001, People's Republic of China

²⁴ Huangshan College, Huangshan 245000, People's Republic of China

²⁵ Hunan Normal University, Changsha 410081, People's Republic of China

²⁶ Hunan University, Changsha 410082, People's Republic of China

- ²⁷ Indian Institute of Technology Madras, Chennai 600036, India
²⁸ Indiana University, Bloomington, Indiana 47405, USA
²⁹ INFN Laboratori Nazionali di Frascati , (A)INFN Laboratori Nazionali di Frascati, I-00044, Frascati, Italy; (B)INFN Sezione di Perugia, I-06100, Perugia, Italy;
(C)University of Perugia, I-06100, Perugia, Italy
³⁰ INFN Sezione di Ferrara, (A)INFN Sezione di Ferrara, I-44122, Ferrara, Italy;
(B)University of Ferrara, I-44122, Ferrara, Italy
³¹ Inner Mongolia University, Hohhot 010021, People's Republic of China
³² Institute of Modern Physics, Lanzhou 730000, People's Republic of China
³³ Institute of Physics and Technology, Mongolian Academy of Sciences, Peace Avenue
54B, Ulaanbaatar 13330, Mongolia
³⁴ Instituto de Alta Investigación, Universidad de Tarapacá, Casilla 7D, Arica 1000000,
Chile
³⁵ Jilin University, Changchun 130012, People's Republic of China
³⁶ Johannes Gutenberg University of Mainz, Johann-Joachim-Becher-Weg 45, D-55099
Mainz, Germany
³⁷ Joint Institute for Nuclear Research, 141980 Dubna, Moscow region, Russia
³⁸ Justus-Liebig-Universitaet Giessen, II. Physikalisches Institut, Heinrich-Buff-Ring 16,
D-35392 Giessen, Germany
³⁹ Lanzhou University, Lanzhou 730000, People's Republic of China
⁴⁰ Liaoning Normal University, Dalian 116029, People's Republic of China
⁴¹ Liaoning University, Shenyang 110036, People's Republic of China
⁴² Nanjing Normal University, Nanjing 210023, People's Republic of China
⁴³ Nanjing University, Nanjing 210093, People's Republic of China
⁴⁴ Nankai University, Tianjin 300071, People's Republic of China
⁴⁵ National Centre for Nuclear Research, Warsaw 02-093, Poland
⁴⁶ North China Electric Power University, Beijing 102206, People's Republic of China
⁴⁷ Peking University, Beijing 100871, People's Republic of China
⁴⁸ Qufu Normal University, Qufu 273165, People's Republic of China
⁴⁹ Renmin University of China, Beijing 100872, People's Republic of China
⁵⁰ Shandong Normal University, Jinan 250014, People's Republic of China
⁵¹ Shandong University, Jinan 250100, People's Republic of China
⁵² Shanghai Jiao Tong University, Shanghai 200240, People's Republic of China
⁵³ Shanxi Normal University, Linfen 041004, People's Republic of China
⁵⁴ Shanxi University, Taiyuan 030006, People's Republic of China
⁵⁵ Sichuan University, Chengdu 610064, People's Republic of China
⁵⁶ Soochow University, Suzhou 215006, People's Republic of China
⁵⁷ South China Normal University, Guangzhou 510006, People's Republic of China
⁵⁸ Southeast University, Nanjing 211100, People's Republic of China
⁵⁹ State Key Laboratory of Particle Detection and Electronics, Beijing 100049, Hefei
230026, People's Republic of China
⁶⁰ Sun Yat-Sen University, Guangzhou 510275, People's Republic of China
⁶¹ Suranaree University of Technology, University Avenue 111, Nakhon Ratchasima

30000, Thailand

⁶² Tsinghua University, Beijing 100084, People's Republic of China

⁶³ Turkish Accelerator Center Particle Factory Group, (A)Istinye University, 34010, Istanbul, Turkey; (B)Near East University, Nicosia, North Cyprus, 99138, Mersin 10, Turkey

⁶⁴ University of Bristol, H H Wills Physics Laboratory, Tyndall Avenue, Bristol, BS8 1TL, UK

⁶⁵ University of Chinese Academy of Sciences, Beijing 100049, People's Republic of China

⁶⁶ University of Groningen, NL-9747 AA Groningen, The Netherlands

⁶⁷ University of Hawaii, Honolulu, Hawaii 96822, USA

⁶⁸ University of Jinan, Jinan 250022, People's Republic of China

⁶⁹ University of Manchester, Oxford Road, Manchester, M13 9PL, United Kingdom

⁷⁰ University of Muenster, Wilhelm-Klemm-Strasse 9, 48149 Muenster, Germany

⁷¹ University of Oxford, Keble Road, Oxford OX13RH, United Kingdom

⁷² University of Science and Technology Liaoning, Anshan 114051, People's Republic of China

⁷³ University of Science and Technology of China, Hefei 230026, People's Republic of China

⁷⁴ University of South China, Hengyang 421001, People's Republic of China

⁷⁵ University of the Punjab, Lahore-54590, Pakistan

⁷⁶ University of Turin and INFN, (A)University of Turin, I-10125, Turin, Italy;
(B)University of Eastern Piedmont, I-15121, Alessandria, Italy; (C)INFN, I-10125, Turin, Italy

⁷⁷ Uppsala University, Box 516, SE-75120 Uppsala, Sweden

⁷⁸ Wuhan University, Wuhan 430072, People's Republic of China

⁷⁹ Yantai University, Yantai 264005, People's Republic of China

⁸⁰ Yunnan University, Kunming 650500, People's Republic of China

⁸¹ Zhejiang University, Hangzhou 310027, People's Republic of China

⁸² Zhengzhou University, Zhengzhou 450001, People's Republic of China

^a Deceased

^b Also at the Moscow Institute of Physics and Technology, Moscow 141700, Russia

^c Also at the Novosibirsk State University, Novosibirsk, 630090, Russia

^d Also at the NRC "Kurchatov Institute", PNPI, 188300, Gatchina, Russia

^e Also at Goethe University Frankfurt, 60323 Frankfurt am Main, Germany

^f Also at Key Laboratory for Particle Physics, Astrophysics and Cosmology, Ministry of Education; Shanghai Key Laboratory for Particle Physics and Cosmology; Institute of Nuclear and Particle Physics, Shanghai 200240, People's Republic of China

^g Also at Key Laboratory of Nuclear Physics and Ion-beam Application (MOE) and Institute of Modern Physics, Fudan University, Shanghai 200443, People's Republic of China

^h Also at State Key Laboratory of Nuclear Physics and Technology, Peking University, Beijing 100871, People's Republic of China

- ⁱ Also at School of Physics and Electronics, Hunan University, Changsha 410082, China
^j Also at Guangdong Provincial Key Laboratory of Nuclear Science, Institute of Quantum Matter, South China Normal University, Guangzhou 510006, China
^k Also at MOE Frontiers Science Center for Rare Isotopes, Lanzhou University, Lanzhou 730000, People's Republic of China
^l Also at Lanzhou Center for Theoretical Physics, Lanzhou University, Lanzhou 730000, People's Republic of China
^m Also at the Department of Mathematical Sciences, IBA, Karachi 75270, Pakistan
ⁿ Also at Ecole Polytechnique Federale de Lausanne (EPFL), CH-1015 Lausanne, Switzerland
^o Also at Helmholtz Institute Mainz, Staudinger Weg 18, D-55099 Mainz, Germany
^p Also at Hangzhou Institute for Advanced Study, University of Chinese Academy of Sciences, Hangzhou 310024, China

E-mail: besiii-publications@ihep.ac.cn

ABSTRACT: Using 20.3 fb^{-1} of e^+e^- collision data collected at a center-of-mass energy of 3.773 GeV with the BESIII detector, we present improved measurements of the absolute branching fractions of the doubly Cabibbo-suppressed decays $D^+ \rightarrow K^+\pi^0$, $D^+ \rightarrow K^+\eta$ and $D^+ \rightarrow K^+\eta'$ with the double-tag method. The statistical significance of each signal decay exceeds 10σ . The branching fractions are determined to be $\mathcal{B}(D^+ \rightarrow K^+\pi^0) = (1.45 \pm 0.06 \pm 0.06) \times 10^{-4}$, $\mathcal{B}(D^+ \rightarrow K^+\eta) = (1.17 \pm 0.10 \pm 0.03) \times 10^{-4}$ and $\mathcal{B}(D^+ \rightarrow K^+\eta') = (1.88 \pm 0.15 \pm 0.06) \times 10^{-4}$, where the first uncertainties are statistical and the second systematic. These results are consistent with the world average values but with significantly improved precision.

Contents

1	Introduction	2
2	BESIII detector and Monte Carlo simulation	2
3	Measurement method and single tag yields	3
4	Signal yields and Branching fractions	5
5	Systematic uncertainty	6
6	Summary	9
7	Acknowledgement	10

1 Introduction

Studies of doubly Cabibbo-suppressed (DCS) decays of charmed mesons are important for the understanding of charmed hadron dynamics. In theory, the branching fractions (BFs) of the two-body decays $D \rightarrow PP$ and $D \rightarrow VP$, where V and P denote vector and pseudoscalar mesons, respectively, can be calculated by incorporating quark SU(3)-flavor symmetry and symmetry breaking as well as charge-parity (CP) violation [1–6]. These decay amplitudes are typically decomposed using topology amplitudes [7]. Compared to Cabibbo-favored and singly Cabibbo-suppressed D decays, experimental information on DCS decays $D \rightarrow PP$ remains limited. Improved measurements of the BFs of these decays are able to provide valuable insights into charmed meson decays [1–7].

Previous measurements by CLEO, Belle, BaBar, and BESIII [8–12] have determined the BFs of the DCS decays $D^+ \rightarrow K^+\pi^0$, $D^+ \rightarrow K^+\eta$ and $D^+ \rightarrow K^+\eta'$. Both CLEO and BESIII measurements are based on $\psi(3770)$ data with single-tag (ST) method which suffers from high backgrounds, while Belle and BaBar employed relative methods with data on and near the $\Upsilon(4S)$ resonance [9, 10].

This paper reports improved measurements of the absolute BFs of the DCS decays $D^+ \rightarrow K^+\pi^0$, $D^+ \rightarrow K^+\eta$ and $D^+ \rightarrow K^+\eta'$ using the double-tag (DT) method [13]. Charge-conjugated decays are implied. This work is performed by using 20.3 fb^{-1} of e^+e^- collision data [14] collected with the BESIII detector at a center-of-mass energy of $\sqrt{s} = 3.773 \text{ GeV}$. This energy corresponds to the $\psi(3770)$ resonance, which predominantly decays into $D\bar{D}$ (D denotes D^0 or D^+) pairs. The D and \bar{D} mesons are produced without accompanying hadron(s), thereby offering an ideal environment to study D meson decays with the DT technique.

2 BESIII detector and Monte Carlo simulation

The BESIII detector [15] records symmetric e^+e^- collisions provided by the BEPCII storage ring [16] in the center-of-mass energy range from 1.84 to 4.95 GeV, with a peak luminosity of $1.1 \times 10^{33} \text{ cm}^{-2}\text{s}^{-1}$ achieved at $\sqrt{s} = 3.773 \text{ GeV}$. The cylindrical core of the BESIII detector covers 93% of the full solid angle and consists of a helium-based multilayer drift chamber (MDC), a plastic scintillator time-of-flight system (TOF), and a CsI(Tl) electromagnetic calorimeter (EMC), which are all enclosed in a superconducting solenoidal magnet providing a 1.0 T magnetic field. The solenoid is supported by an octagonal flux-return yoke with resistive plate counter muon identification modules interleaved with steel. The charged-particle momentum resolution at $1 \text{ GeV}/c$ is 0.5%, and the dE/dx resolution is 6% for electrons from Bhabha scattering. The EMC measures photon energies with a resolution of 2.5% (5%) at 1 GeV in the barrel (end cap) region. The time resolution in the TOF barrel region is 68 ps, while that in the end cap region was 110 ps. The end-cap TOF system was upgraded in 2015 using multi-gap resistive plate chamber technology, providing a time resolution of 60 ps [17], which benefits about 85% of the data used in this analysis. Details about the design and performance of the BESIII detector are given in Ref. [15].

Simulated samples produced with a GEANT4-based [18] Monte Carlo (MC) package, which includes the geometric description of the BESIII detector and the detector response, are used to determine the detection efficiency and to estimate backgrounds. The simulation includes the beam energy spread and initial state radiation (ISR) in the e^+e^- annihilations modeled with the generator KKMC [19]. The signal decays $D^+ \rightarrow K^+\pi^0$, $D^+ \rightarrow K^+\eta$ and $D^+ \rightarrow K^+\eta'$ are simulated to distribute uniformly in the available phase space. The decays $\eta' \rightarrow \pi^+\pi^-\eta$ and $\eta' \rightarrow \pi^+\pi^-\gamma$ are simulated by using a specific generator developed with the amplitude analysis result [20]. The background is studied using an inclusive MC sample that consists of the production of $D\bar{D}$ pairs with consideration of quantum coherence for all neutral D modes, the non- $D\bar{D}$ decays of the $\psi(3770)$, the ISR production of the J/ψ and $\psi(3686)$ states, and the continuum processes incorporated in KKMC. The known decay modes are modeled with EVTGEN [20] using the known BFs taken from the Particle Data Group (PDG) [12], while the remaining unknown decays from the charmonium states are modeled with LUNDCHARM [21]. Final state radiation from charged final state particles is incorporated with the PHOTOS package [22].

3 Measurement method and single tag yields

Signal D^+ decays are reconstructed in events where D^- decays are also reconstructed through three hadronic decay modes: $D^- \rightarrow K^+\pi^-\pi^-$, $D^- \rightarrow K_S^0\pi^-$, and $D^- \rightarrow K^+\pi^-\pi^-\pi^0$. The K_S^0 and π^0 candidates are reconstructed via $K_S^0 \rightarrow \pi^+\pi^-$ and $\pi^0 \rightarrow \gamma\gamma$, respectively. Selection criteria for K^\pm , π^\pm , K_S^0 and π^0 follow Ref. [23]. If a D^- meson is found, it is referred to as an ST candidate. An event in which a signal D^+ decay and an ST D^- are simultaneously reconstructed is referred to as a DT event. The BF of the signal decay is determined as

$$\mathcal{B}(\text{sig}) = \frac{N_{\text{DT}}}{\sum_{i=1}^3 N_{\text{ST}}^i (\epsilon_{\text{DT}}^i / \epsilon_{\text{ST}}^i)}, \quad (3.1)$$

where N_{DT} is the number of DT events, ϵ_{DT}^i is the efficiency of detecting DT events including the sub-BFs, N_{ST}^i is the number of ST D^- mesons, ϵ_{ST}^i is the corresponding ST efficiency for the i -th tag mode.

The tagged D^- mesons are selected using two variables: the energy difference

$$\Delta E_{\text{tag}} \equiv E_{D^-} - E_b, \quad (3.2)$$

and the beam-constrained mass

$$M_{\text{BC}}^{\text{tag}} \equiv \sqrt{E_b^2 - |\vec{p}_{D^-}|^2}, \quad (3.3)$$

where E_b is the beam energy, and \vec{p}_{D^-} and E_{D^-} candidates are the momentum and the energy of the D^- candidate in the e^+e^- rest frame. For each tag mode, if there are multiple combinations, the one with the minimum $|\Delta E_{\text{tag}}|$ is retained for further analysis. For the tag modes $D^- \rightarrow K^+\pi^-\pi^-$, $D^- \rightarrow K_S^0\pi^-$ and $D^- \rightarrow K^+\pi^-\pi^-\pi^0$, the tagged D^- candidates are required to satisfy $\Delta E_{\text{tag}} \in (-25, 24)$, $(-25, 25)$ and $(-57, 46)$ MeV,

Table 1. Requirement of ΔE , ST D^- yields in data and ST efficiencies (ϵ_{ST}) [23].

Tag mode	ΔE (MeV)	$N_{\text{ST}} (\times 10^3)$	$\epsilon_{\text{ST}} (\%)$
$K^+\pi^-\pi^-$	[-25, 24]	5526.6 ± 2.5	51.07
$K_S^0\pi^-$	[-25, 26]	656.5 ± 0.8	51.42
$K^+\pi^-\pi^-\pi^0$	[-57, 46]	1740.2 ± 1.8	24.53

respectively. The yields of ST D^- mesons are obtained from maximum likelihood fits to the $M_{\text{BC}}^{\text{tag}}$ distributions of the accepted ST candidates, as shown in Table 1. The fit results are shown in Fig. 1. The total ST D^- yield is $N_{\text{ST}} = (8131.7 \pm 3.3) \times 10^3$.

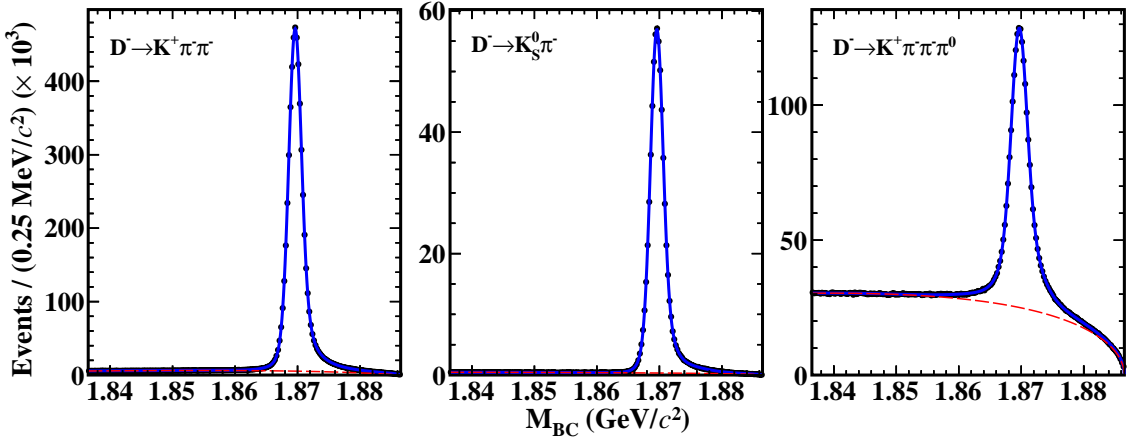


Figure 1. Fits to the M_{BC} distributions of the ST D^- candidates. The dots with error bars are data, and the blue solid and red dashed curves are the fit results and the fitted backgrounds, respectively.

The signal D^+ candidates are reconstructed from the particles used in the tagged D^- reconstruction. The K_S^0 , π^0 and η candidates are reconstructed via the decays $K_S^0 \rightarrow \pi^+\pi^-$, $\pi^0 \rightarrow \gamma\gamma$ and $\eta \rightarrow \gamma\gamma$, respectively. The selection criteria for K^\pm , π^\pm , K_S^0 , π^0 and η are the same as those in Ref. [23]. The η' signal regions are defined as $|M_{\pi^+\pi^-\eta} - 0.958| < 0.012$ GeV/ c^2 and $|M_{\pi^+\pi^-\gamma} - 0.958| < 0.020$ GeV/ c^2 . The corresponding sideband regions are $0.020 < |M_{\pi^+\pi^-\eta} - 0.958| < 0.044$ GeV/ c^2 and $0.030 < |M_{\pi^+\pi^-\gamma} - 0.958| < 0.070$ GeV/ c^2 .

The energy difference (ΔE_{sig}) and beam-constrained mass ($M_{\text{BC}}^{\text{sig}}$) are used to select signal D^+ candidates. These quantities are calculated similarly to Eqs. (3.2) and (3.3), respectively, with D^- replaced by D^+ . If there are multiple combinations, primarily due to incorrect π^0 reconstruction, the combination with the minimum $|\Delta E_{\text{sig}}|$ is retained for further analysis. The signal side is required to satisfy $\Delta E_{\text{sig}} \in (-72, 49), (-43, 41), (-32, 31)$ and $(-43, 40)$ MeV for $D^+ \rightarrow K^+\pi^0$, $D^+ \rightarrow K^+\eta$, $D^+ \rightarrow K^+\eta'_{\pi^+\pi^-\eta}$ and $D^+ \rightarrow K^+\eta'_{\pi^+\pi^-\gamma}$.

To suppress non- D^+D^- events, the opening angle between the D^+ and D^- candidates is required to be greater than 160° . The top-left panels of Figs. 2 and 3 show the $M_{\text{BC}}^{\text{tag}}$ versus $M_{\text{BC}}^{\text{sig}}$ distributions of the accepted candidates for $D^+ \rightarrow K^+\pi^0$, $D^+ \rightarrow K^+\eta$, $D^+ \rightarrow K^+\eta'_{\pi^+\pi^-\eta}$ and $D^+ \rightarrow K^+\eta'_{\pi^+\pi^-\gamma}$ in data.

Additionally, $D^+ \rightarrow K^+\pi^0$ candidates are required to have no additional π^0 meson to suppress the peaking background from $D^+ \rightarrow \pi^+\pi^0\pi^0$. To further reject possible K_S^0 background, a veto window $|M_{\pi^+\pi^-} - 0.498| > 0.012 \text{ GeV}/c^2$ is applied for $D^+ \rightarrow K^+\eta'(\pi^+\pi^-\gamma)$ candidates.

4 Signal yields and Branching fractions

The yields of DT events are extracted from a two-dimensional (2D) unbinned maximum likelihood fit to the corresponding distribution of $M_{\text{BC}}^{\text{tag}}$ versus $M_{\text{BC}}^{\text{sig}}$ [24–26]. The signal shape is described by a 2D probability density function (PDF) from the MC simulation after convolving with a Gaussian resolution function with parameters derived from data. For various background components, the individual PDFs are constructed as follows: [24–26]

- BKGI: $b(x) \cdot c_y(y; E_b, \xi_y) + b(y) \cdot c_x(x; E_b, \xi_x)$,
- BKGII: $c_z(z; \sqrt{2}E_b, \xi_z) \cdot g(k; 0, \sigma_k)$,
- BKGIII: $c_x(x; E_b, \xi_x) \cdot c_y(y; E_b, \xi_y)$.

Here, $x = M_{\text{BC}}^{\text{tag}}$, $y = M_{\text{BC}}^{\text{sig}}$, $z = (x + y)/\sqrt{2}$, and $k = (x - y)/\sqrt{2}$. The functions $b(x)$ and $b(y)$ are the one-dimensional signal shapes taken from the MC simulation. The function c_f is an ARGUS function [27] defined as

$$c_f(f; E_b, \xi_f) = A_f f \left(1 - \frac{f^2}{E_b^2}\right)^{\frac{1}{2}} e^{\xi_f(1 - \frac{f^2}{E_b^2})}, \quad (4.1)$$

where f denotes x , y , or z , E_b is fixed at 1.8865 GeV, A_f is a normalization factor, and ξ_f is a fit parameter. The function $g(k; \sigma_k)$ is a Gaussian distribution with a mean of zero and a standard deviation $\sigma_k = \sigma_0 \cdot (\sqrt{2}E_b - z)^p$, where σ_0 and p are free parameters in the fit. All other parameters are left free to vary. The three types of background are illustrated as one curve in Figs. 2 and 3. For $D^+ \rightarrow K^+\pi^0$, the peaking background yield, including $\pi^+\pi^0$ and $K_S^0\pi^+$, is fixed at the value estimated from the inclusive MC samples. Furthermore, for $D^+ \rightarrow K^+\eta'(\pi^+\pi^-\eta)$ and $D^+ \rightarrow K^+\eta'(\pi^+\pi^-\gamma)$, a simultaneous fit is performed to extract the BF as a shared parameter. The contribution from the $D^+ \rightarrow K^+\eta'(\pi^+\pi^-\gamma)$ sideband regions is re-normalized to the signal regions. The contribution from the $D^+ \rightarrow K^+\eta'(\pi^+\pi^-\eta)$ sideband regions is neglected since only one event survives after event selection.

The spectra in the middle and right columns in Figs. 2 and 3 show the projections on $M_{\text{BC}}^{\text{tag}}$ and $M_{\text{BC}}^{\text{sig}}$ of the 2D fits to data. For each signal decay, the statistical significance is evaluated as $\sqrt{-2 \ln(\mathcal{L}_0/\mathcal{L}_{\max})}$, where \mathcal{L}_{\max} is the maximum likelihood of the nominal fit and \mathcal{L}_0 is the likelihood of the fit without including the signal. The change of the number of degrees of freedom is assumed to be 5 for $K^+\pi^0$ and $K^+\eta$ decay mode, representing the signal yield. The change of the number of degrees of freedom is assumed to be 7 for $K^+\eta'$, representing the signal yield of $K^+\eta'(\pi^+\pi^-\eta)$, the signal yield of $K^+\eta'(\pi^+\pi^-\gamma)$ and the shared parameter for the BF of $D^+ \rightarrow K^+\eta'$. The statistical significance of each signal

Table 3. The numbers used in the BF calculations, where the uncertainties are statistical only. N_{DT} is the fitted numbers of the DT events in data, $\epsilon_{\text{DT}}/\epsilon_{\text{ST}}$ is the efficiency of detecting the signal decay in the presence of the ST D^- , which includes BFs of the intermediate states. \mathcal{B}_{sig} is the BF of signal decay.

Signal decay	$D^+ \rightarrow K^+\pi^0$	$D^+ \rightarrow K^+\eta$	$D^+ \rightarrow K^+\eta'$
N_{DT}	629 ± 28	182 ± 15	214 ± 17
$\epsilon_{\text{DT}}/\epsilon_{\text{ST}} (\%)$	53.29 ± 0.36	19.20 ± 0.13	14.02 ± 0.11
$\mathcal{B}_{\text{sig}} (\times 10^{-4})$	1.45 ± 0.06	1.17 ± 0.10	1.88 ± 0.15

decay exceeds 10σ . The detailed ST, DT and DT/ST efficiencies are shown in Table. 2. The signal yields in data, the detection efficiencies, and the obtained BFs of each signal decay are summarized in Table 3.

Table 2. The efficiencies ϵ_{ST}^i , ϵ_{DT}^i and $\epsilon_{\text{DT}}^i/\epsilon_{\text{ST}}^i$ which includes BFs of the intermediate states. The uncertainties are statistical only.

Tag mode	$\epsilon_{\text{ST}}^i (\%)$	ϵ_{DT}^i for $D^+ \rightarrow K^+\pi^0$ (%)	$\epsilon_{\text{DT}}^i/\epsilon_{\text{ST}}^i$ for $D^+ \rightarrow K^+\pi^0$ (%)
$D^- \rightarrow K^+\pi^-\pi^-$	51.07 ± 0.01	27.23 ± 0.17	53.31 ± 0.33
$D^- \rightarrow K_S^0\pi^-$	51.42 ± 0.01	27.75 ± 0.17	53.97 ± 0.33
$D^- \rightarrow K^+\pi^-\pi^-\pi^0$	24.53 ± 0.01	12.84 ± 0.12	52.36 ± 0.49
Weight	53.29 ± 0.36		
Tag mode	$\epsilon_{\text{ST}}^i (\%)$	ϵ_{DT}^i for $D^+ \rightarrow K^+\eta$ (%)	$\epsilon_{\text{DT}}^i/\epsilon_{\text{ST}}^i$ for $D^+ \rightarrow K^+\eta$ (%)
$D^- \rightarrow K^+\pi^-\pi^-$	51.07 ± 0.01	9.83 ± 0.06	19.24 ± 0.12
$D^- \rightarrow K_S^0\pi^-$	51.42 ± 0.01	9.95 ± 0.06	19.36 ± 0.12
$D^- \rightarrow K^+\pi^-\pi^-\pi^0$	24.53 ± 0.01	4.59 ± 0.04	18.72 ± 0.18
Weight	19.20 ± 0.13		
Tag mode	$\epsilon_{\text{ST}}^i (\%)$	ϵ_{DT}^i for $D^+ \rightarrow K^+\eta'$ (%)	$\epsilon_{\text{DT}}^i/\epsilon_{\text{ST}}^i$ for $D^+ \rightarrow K^+\eta'$ (%)
$D^- \rightarrow K^+\pi^-\pi^-$	51.07 ± 0.01	7.28 ± 0.05	14.26 ± 0.10
$D^- \rightarrow K_S^0\pi^-$	51.42 ± 0.01	7.53 ± 0.05	14.64 ± 0.11
$D^- \rightarrow K^+\pi^-\pi^-\pi^0$	24.53 ± 0.01	2.99 ± 0.03	12.21 ± 0.14
Weight	14.02 ± 0.11		

5 Systematic uncertainty

With the DT method, most of the uncertainties related to the ST selection cancel out. The systematic uncertainties arise from the following sources and are estimated relative to the measured BFs.

The uncertainty of the total ST D^- yield is due to the fit to the $M_{\text{BC}}^{\text{tag}}$ distributions and is assigned as 0.3% [28].

The tracking or particle identification (PID) efficiencies of K^+ and π^\pm are estimated by analyzing DT $D^+ \rightarrow K^-\pi^+\pi^+$ versus $D^- \rightarrow K^+\pi^-\pi^-$ hadronic events. The systematic uncertainties in the tracking or PID are assigned as 1.0% per track [29].

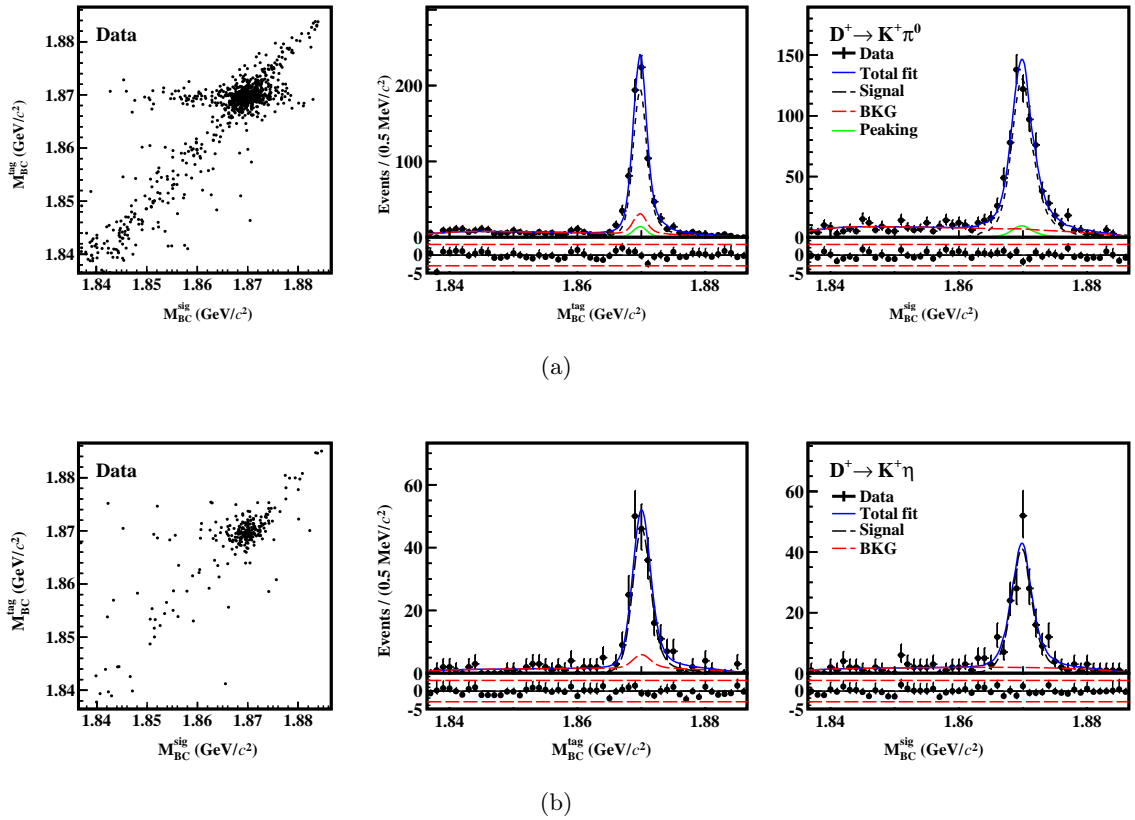


Figure 2. The distributions of M_{BC}^{tag} versus M_{BC}^{sig} and the projections on M_{BC}^{sig} and M_{BC}^{tag} of the 2D fits to the DT candidate events of (a) $D^+ \rightarrow K^+\pi^0$ and (b) $D^+ \rightarrow K^+\eta$ in data sample with three tags. For both sub-figures (a) and (b), in the right two columns, the dots with error bars are data, the blue solid curves are the fit results, the black dashed lines are the signals, and the red dashed lines are the BKG I, II and III. For sub-figure (a), the green dashed line is fixed peaking background.

The systematic uncertainty of the γ selection is estimated by studying the control sample of $J/\psi \rightarrow \pi^0\pi^+\pi^-$ [30]. The systematic uncertainty in the γ selection is assigned as 1.0% per photon.

The systematic uncertainty of the π^0 reconstruction has been well studied by using the DT $\bar{D}^0 \rightarrow K^+\pi^-$ versus $D^0 \rightarrow K^-\pi^+\pi^0$ events. We assign the systematic uncertainty in the π^0 reconstruction to be 2.0% per π^0 [29]. Due to limited η sample, the systematic uncertainty of the η reconstruction is assigned as 2.0% per η by referring to that of π^0 .

The systematic uncertainty of the η' mass window has been studied in $D^+ \rightarrow \eta'\ell^+\nu_\ell$ [31]. The systematic uncertainty due to the η' mass window is assigned as 0.7% [31].

The uncertainties of the quoted BFs of $\pi^0 \rightarrow \gamma\gamma$, $\eta \rightarrow \gamma\gamma$, $\eta' \rightarrow \pi^+\pi^-\eta$ and $\eta' \rightarrow \pi^+\pi^-\gamma$ are 0.03%, 0.5%, 1.2% and 1.4%, respectively [12].

The systematic uncertainty of the ΔE^{sig} requirement is estimated with the control samples of $D^+ \rightarrow \pi^+\pi^0$, $D^+ \rightarrow \pi^+\eta$, $D^+ \rightarrow \pi^+\eta'_{\pi^+\pi^-\eta}$ and $D^+ \rightarrow \pi^+\eta'_{\pi^+\pi^-\gamma}$. The

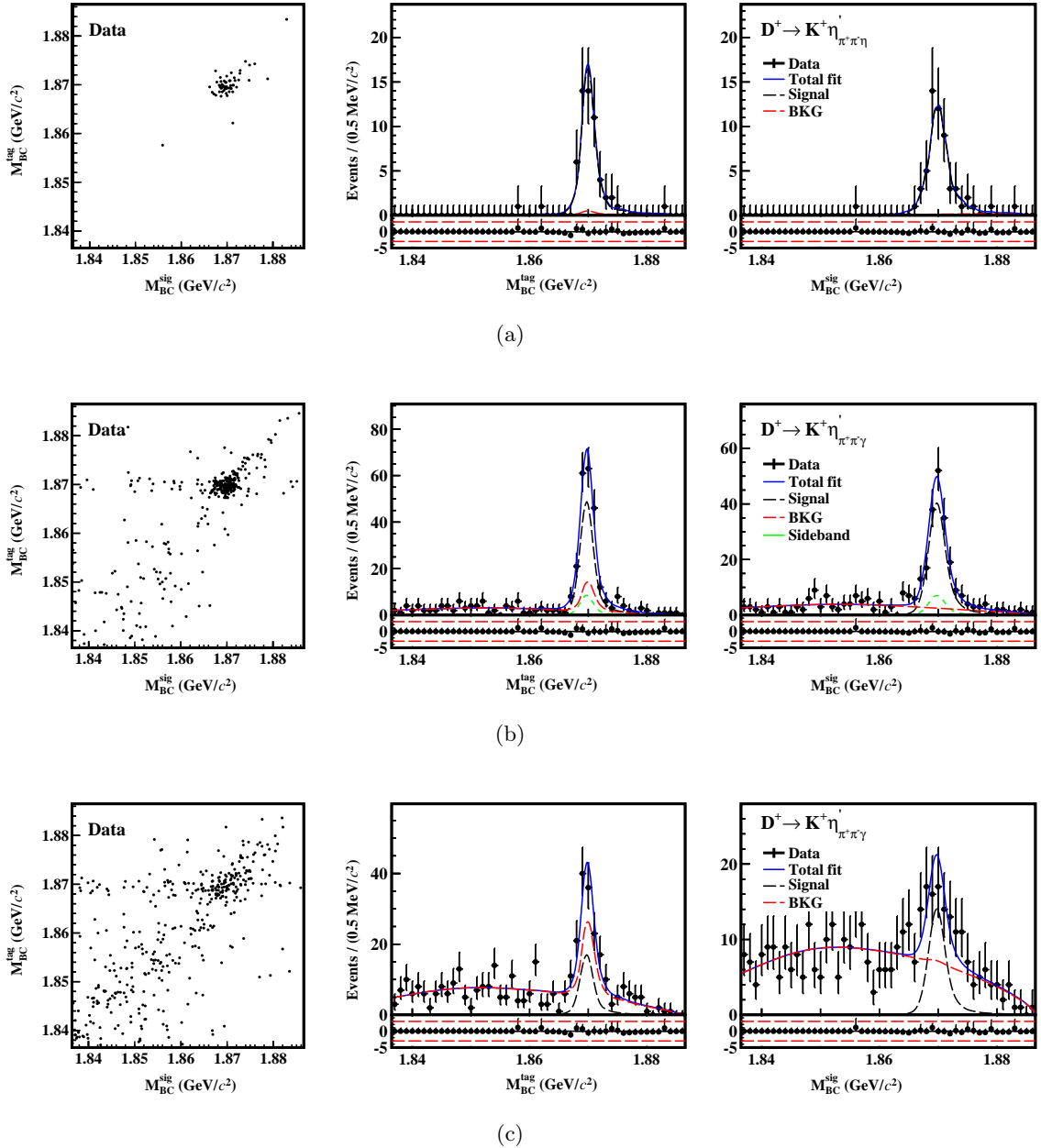


Figure 3. The distributions of M_{BC}^{tag} versus M_{BC}^{sig} and the projections on M_{BC}^{sig} and M_{BC}^{tag} of the 2D fits to the DT candidate events of (a) $D^+ \rightarrow K^+ \eta'(\pi^+ \pi^- \eta)$, (b) $D^+ \rightarrow K^+ \eta'(\pi^+ \pi^- \gamma)$ in the η' signal region and (c) $D^+ \rightarrow K^+ \eta'(\pi^+ \pi^- \gamma)$ in the η' sideband region in data sample with three tags. In the fit of (c), the parameters of the smeared Gaussian function have been fixed to those in the η' signal region. For all three sub-figures (a), (b) and (c), in the right two columns, the dots with error bars are data, the blue solid curves are the fit results, the black dashed lines are the signals, and the red dashed lines are the BKG I, II and III. For sub-figure (b), the green dashed line is the normalized sideband events. For sub-figure (a), due to the low backgrounds, the black curves overlap with blue curves.

differences in acceptance efficiencies between data and inclusive MC sample are taken as the systematic uncertainties. They are 1.1%, 0.4%, 0.1% and 0.1% for $D^+ \rightarrow K^+\pi^0$, $D^+ \rightarrow K^+\eta$, $D^+ \rightarrow K^+\eta'_{\pi^+\pi^-\eta}$ and $D^+ \rightarrow K^+\eta'_{\pi^+\pi^-\gamma}$, respectively.

The systematic uncertainties of the 2D fit are mainly due to signal shapes, background shapes, and peaking background. The uncertainties due to signal shapes are estimated by using the MC shapes without convolving with Gaussian resolution. The uncertainties due to the background shapes are estimated by varying the endpoint by $0.2 \text{ MeV}/c^2$ for the ARGUS function. The systematic uncertainties due to peaking background are estimated by varying the BFs of the peaking background channels by $\pm 1\sigma$ [12]. After adding these three uncertainties in quadrature, the systematic uncertainties of the 2D fit are assigned to be 0.5%, 0.3%, 1.5% and 1.5% for $D^+ \rightarrow K^+\pi^0$, $D^+ \rightarrow K^+\eta$, $D^+ \rightarrow K^+\eta'_{\pi^+\pi^-\eta}$ and $D^+ \rightarrow K^+\eta'_{\pi^+\pi^-\gamma}$, respectively.

The systematic uncertainty of K_S^0 veto is estimated by examining the BFs after enlarging the veto window by ± 10 and $\pm 20 \text{ MeV}/c^2$. The change of the re-measured BF, 1.8%, is assigned for $D^+ \rightarrow K^+\eta'$.

The systematic uncertainty of fit bias is estimated with 40 times fake data, each with an equivalent size to the data. The difference between the fit mean value of the 40 times fake data and the input value, 3.0%, is taken as systematic uncertainty for $D^+ \rightarrow K^+\pi^0$. The systematic uncertainty is negligible for other signal decays.

The systematic uncertainties due to the D^+D^- opening angle requirement are estimated by using the control samples of $D^+ \rightarrow \pi^+\pi^0$, $D^+ \rightarrow \pi^+\eta$, $D^+ \rightarrow \pi^+\eta'_{\pi^+\pi^-\eta}$ and $D^+ \rightarrow \pi^+\eta'_{\pi^+\pi^-\gamma}$. The differences in the acceptance efficiencies between data and MC simulation are assigned as individual systematic uncertainties, which are 1.3%, 0.2%, 2.8% and 1.9% for $D^+ \rightarrow K^+\pi^0$, $D^+ \rightarrow K^+\eta$, $D^+ \rightarrow K^+\eta'_{\pi^+\pi^-\eta}$ and $D^+ \rightarrow K^+\eta'_{\pi^+\pi^-\gamma}$, respectively.

By adding each of the systematic uncertainties in quadrature, we obtain the total systematic uncertainties for $D^+ \rightarrow K^+\pi^0$, $D^+ \rightarrow K^+\eta$, $D^+ \rightarrow K^+\eta'_{\pi^+\pi^-\eta}$ and $D^+ \rightarrow K^+\eta'_{\pi^+\pi^-\gamma}$, respectively. All these systematic uncertainties are summarized in Table 4. For $D^+ \rightarrow K^+\eta'_{\pi^+\pi^-\eta}$ and $D^+ \rightarrow K^+\eta'_{\pi^+\pi^-\gamma}$, the correlated systematic uncertainties including those of total ST D^- yield, $K^+(\pi^\pm)$ PID or tracking, η' mass window and 2D fit; the total effect of these sources is 2.7%. The un-correlated systematic uncertainties are from γ selection, $\pi^0(\eta)$ reconstruction, quoted BFs, ΔE^{sig} , MC statistics, K_S^0 veto, fit bias and opening angle requirement; they are 2.7% and 2.5% for $D^+ \rightarrow K^+\eta'_{\pi^+\pi^-\eta}$ and $D^+ \rightarrow K^+\eta'_{\pi^+\pi^-\gamma}$, respectively. The total systematic uncertainty is obtained to be 3.3% by combining the systematic uncertainties of $D^+ \rightarrow K^+\eta'_{\pi^+\pi^-\eta}$ and $D^+ \rightarrow K^+\eta'_{\pi^+\pi^-\gamma}$ [32].

6 Summary

In summary, using 20.3 fb^{-1} of e^+e^- collision data taken at $\sqrt{s} = 3.773 \text{ GeV}$ with the BESIII detector, we measure the BFs of the DCS decays $D^+ \rightarrow K^+\pi^0$, $D^+ \rightarrow K^+\eta$ and $D^+ \rightarrow K^+\eta'$ to be $\mathcal{B}(D^+ \rightarrow K^+\pi^0) = (1.45 \pm 0.06 \pm 0.06) \times 10^{-4}$, $\mathcal{B}(D^+ \rightarrow K^+\eta) = (1.17 \pm 0.10 \pm 0.03) \times 10^{-4}$ and $\mathcal{B}(D^+ \rightarrow K^+\eta') = (1.88 \pm 0.15 \pm 0.06) \times 10^{-4}$, where the first uncertainties are statistical and the second are systematic. The precision of the BF of $D^+ \rightarrow K^+\pi^0$ is improved by a factor of two compared to the world average, while

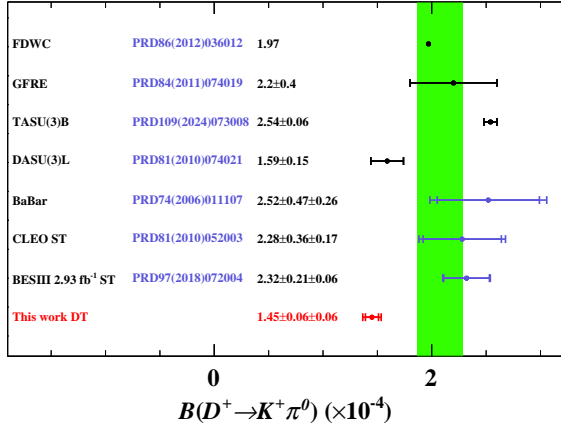
Table 4. Relative systematic uncertainties (%) in the BF measurements. The top and bottom parts are correlated and uncorrelated systematic uncertainties for $D^+ \rightarrow K^+\eta'_{\pi^+\pi^-\eta}$ and $D^+ \rightarrow K^+\eta'_{\pi^+\pi^-\gamma}$, respectively. The "..." means the uncertainty is negligible.

Uncertainty	$D^+ \rightarrow K^+\pi^0$	$D^+ \rightarrow K^+\eta$	$D^+ \rightarrow K^+\eta'_{\pi^+\pi^-\eta}$	$D^+ \rightarrow K^+\eta'_{\pi^+\pi^-\gamma}$
N_{tag}	0.3	0.3	0.3	0.3
$K^+(\pi^\pm)$ tracking	0.5	0.5	1.5	1.5
$K^+(\pi^\pm)$ PID	0.5	0.5	1.5	1.5
η' mass window	0.7	0.7
2D fit	0.5	0.3	1.5	1.5
γ selection	1.0
$\pi^0(\eta)$ reconstruction	2.0	2.0	2.0	...
Quoted \mathcal{B}	0.03	0.4	1.3	1.4
ΔE^{sig} cut	1.1	0.4	0.1	0.1
MC statistics	0.2	0.2	0.3	0.2
K_S^0 veto	1.8
Fit bias	3.0
Opening angle requirement	0.3	0.2	1.3	0.3
Total	3.9	2.2	3.8	3.7

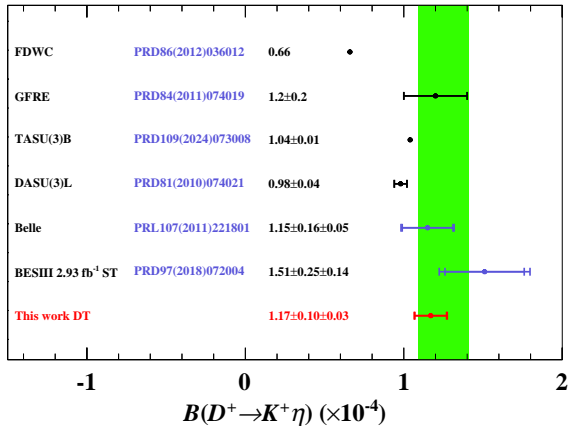
the latter two are comparable with the world averages. We notice that there are about four standard deviations between $\mathcal{B}(D^+ \rightarrow K^+\pi^0)$ measured in this work and that in Ref. [11]. This difference is likely attributable to that the measurement in Ref. [11] used the single-tag method, which suffers from much higher background, and the systematic uncertainty due to background shape could be substantially underestimated. These BFs of $D^+ \rightarrow K^+\pi^0$ and $D^+ \rightarrow K^+\eta$ are consistent with DASU(3)L theoretical predictions [1], while the BFs of $D^+ \rightarrow K^+\pi^0$ and $D^+ \rightarrow K^+\eta'$ are inconsistent with TASU(3)B theoretical predictions [2]. The comparisons of our results with other experimental measurements and theoretical calculations are shown in Table 5 and Fig. 4.

7 Acknowledgement

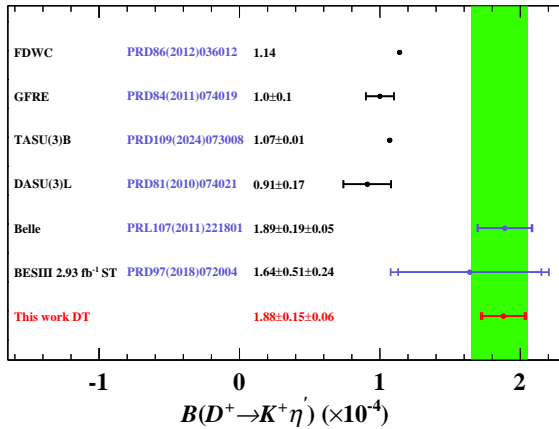
The BESIII Collaboration thanks the staff of BEPCII (<https://cstr.cn/31109.02.BEPC>) and the IHEP computing center for their strong support. This work is supported in part by National Key R&D Program of China under Contracts Nos. 2023YFA1606000, 2023YFA1606704; National Natural Science Foundation of China (NSFC) under Contracts Nos. 12035009, 11635010, 11935015, 11935016, 11935018, 12025502, 12035013, 12061131003, 12192260, 12192261, 12192262, 12192263, 12192264, 12192265, 12221005, 12225509, 12235017, 12361141819; The Chinese Academy of Sciences (CAS) Large-Scale Scientific Facility Program; CAS under Contract No. YSBR-101; 100 Talents Program of CAS; The Institute of Nuclear and Particle Physics (INPAC) and Shanghai Key Laboratory for Particle Physics and Cosmology; Agencia Nacional de Investigación y Desarrollo de Chile (ANID), Chile under Contract No. ANID PIA/APOYO AFB230003; German Research Foundation DFG under Contract No. FOR5327; Istituto Nazionale di Fisica Nucleare, Italy; Knut and Alice Wallenberg Foundation under Contracts Nos. 2021.0174, 2021.0299; Ministry of Development



(a)



(b)



(c)

Figure 4. Comparisons of experimental measurements and theoretical calculations for (a) $D^+ \rightarrow K^+\pi^0$, (b) $D^+ \rightarrow K^+\eta$ and (c) $D^+ \rightarrow K^+\eta'$. The green bands represent the PDG values. For experimental results, the first uncertainties are statistical and the second ones are systematic. For theoretical calculations, the uncertainties are theoretical only.

Table 5. The BFs ($\times 10^{-4}$) of $D^+ \rightarrow K^+\pi^0$, $D^+ \rightarrow K^+\eta$ and $D^+ \rightarrow K^+\eta'$ from experimental measurements and theoretical calculations. For the experimental results, the first uncertainties are statistical and the second ones are systematic. For the theoretical prediction, the uncertainties are theoretical only. The "..." means no this results.

Signal decay	$D^+ \rightarrow K^+\pi^0$	$D^+ \rightarrow K^+\eta$	$D^+ \rightarrow K^+\eta'$
CLEO [8]	$2.28 \pm 0.36 \pm 0.17$
Belle [9]	...	$1.15 \pm 0.16 \pm 0.05$	$1.87 \pm 0.19 \pm 0.05$
BaBar [10]	$2.52 \pm 0.47 \pm 0.26$
BESIII [11]	$2.32 \pm 0.21 \pm 0.06$	$1.51 \pm 0.25 \pm 0.14$	$1.64 \pm 0.51 \pm 0.24$
PDG [12]	2.08 ± 0.21	1.25 ± 0.16	1.85 ± 0.20
DASU(3)L [1]	1.59 ± 0.15	0.98 ± 0.04	0.91 ± 0.17
TASU(3)B [2]	2.54 ± 0.06	1.04 ± 0.01	1.07 ± 0.01
GFRE [3]	2.2 ± 0.4	1.2 ± 0.2	1.0 ± 0.1
FDWC [4]	1.97	0.66	1.14
This work	$1.45 \pm 0.06 \pm 0.06$	$1.17 \pm 0.10 \pm 0.03$	$1.88 \pm 0.15 \pm 0.06$

of Turkey under Contract No. DPT2006K-120470; National Research Foundation of Korea under Contract No. NRF-2022R1A2C1092335; National Science and Technology fund of Mongolia; Polish National Science Centre under Contract No. 2024/53/B/ST2/00975; Swedish Research Council under Contract No. 2019.04595; U. S. Department of Energy under Contract No. DE-FG02-05ER41374.

References

- [1] H. Y. Cheng and C. W. Chiang, *Phys. Rev. D* **81**, 074021 (2010).
- [2] H. Y. Cheng and C. W. Chiang, *Phys. Rev. D* **109**, 073008 (2024).
- [3] F. S. Yu, X. X. Wang, and C.D. Yu, *Phys. Rev. D* **84**, 074019 (2011).
- [4] H. N. Li, C. D. Lu, and F.S. Yu, *Phys. Rev. D* **86**, 036012 (2012).
- [5] H. J. Lipkin, *Phys. Rev. Lett.* **46**, 1307 (1981).
- [6] Y. Grossman and D. J. Robinson, *J. High Energy Phys.* **04**, (2013) 067.
- [7] C. W. Chiang and Jonathan L. Rosner, *Phys. Rev. D* **65**, 054007 (2002).
- [8] H. Mendez *et al.* (CLEO Collaboration), *Phys. Rev. D* **81**, 052013 (2010).
- [9] E. Won *et al.* (Belle Collaboration), *Phys. Rev. Lett.* **107**, 221801 (2011).
- [10] B. Aubert *et al.* (BaBar Collaboration), *Phys. Rev. D* **74**, 011107(R) (2006).
- [11] M. Ablikim *et al.* (BESIII Collaboration), *Phys. Rev. D* **97**, 072004 (2018).
- [12] S. Navas *et al.* (Particle Data Group), *Phys. Rev. D* **110**, 030001 (2024).
- [13] R. M. Baltrusaitis *et al.* (MARK III Collaboration), *Phys. Rev. Lett.* **56**, 2140 (1986); J. Adler *et al.* (MARK III Collaboration), *Phys. Rev. Lett.* **60**, 89 (1988).
- [14] M. Ablikim *et al.* (BESIII Collaboration), *Chin. Phys. C* **48**, 123001(2024)
- [15] M. Ablikim *et al.* (BESIII Collaboration), *Nucl. Instrum. Meth. A* **614**, 345 (2010).

- [16] C. H. Yu *et al.*, Proceeding of IPAC 2016, Bosan, Korea, 2016.
- [17] X. Li *et al.*, Radiat. Detect. Technol. Methods **1**, 13 (2017).
- [18] S. Agostinelli *et al.* (GEANT4 Collaboration), Nucl. Instrum. Meth. A **506**, 250 (2003).
- [19] S. Jadach, B. F. L. Ward, and Z. Was, Phys. Rev. D **63**, 113009 (2001);
- [20] D. J. Lange, Nucl. Instrum. Meth. A **462**, 152 (2001); R. G. Ping, Chin. Phys. C **32**, 599 (2008). Comput. Phys. Commun. **130**, 260 (2000).
- [21] J. C. Chen, G. S. Huang, X. R. Qi, D. H. Zhang, and Y. S. Zhu, Phys. Rev. D **62**, 034003 (2000).
- [22] E. Richter-Was, Phys. Lett. B **303**, 163 (1993).
- [23] M. Ablikim *et al.* (BESIII Collaboration), Phys. Rev. D **109**, 072003 (2024).
- [24] S. Dobbs *et al.* (CLEO Collaboration), Phys. Rev. D. **76**, 112001 (2007).
- [25] M. Ablikim *et al.* (BESIII Collaboration), Phys. Rev. D. **105**, 112001 (2022).
- [26] M. Ablikim *et al.* (BESIII Collaboration), Phys. Rev. D. **125**, 141802 (2020).
- [27] H. Albrecht *et al.* (ARGUS Collaboration), Phys. Lett. B **241**, 278 (1990).
- [28] M. Ablikim *et al.* (BESIII Collaboration), Phys. Rev. D **109**, 072003 (2024).
- [29] M. Ablikim *et al.* (BESIII Collaboration), J. High Energy Phys. 09 (2024) 107.
- [30] M. Ablikim *et al.* (BESIII Collaboration), Phys. Rev. D **83**, 112005 (2011).
- [31] M. Ablikim *et al.* (BESIII Collaboration), Phys. Rev. Lett. **134**, 111801 (2025).
- [32] M. Ablikim *et al.* (BESIII Collaboration), Phys. Rev. D **110**, 072017 (2024).